

Growth-Rate-Dependent Properties of GaSb/GaAs Quantum Dots on (001) Ge Substrate by Molecular Beam Epitaxy

Zon, Pakawat Phienlumert, Supachok Thainoi, Suwit Kiravittaya,*
Aniwat Tandaechanurat, Noppadon Nuntawong, Suwat Sopitpan, Visittapong Yordsri,
Chanchana Thanachayanont, Songphol Kanjanachuchai, Somchai Ratanathamphan,
Somsak Panyakeow,* Yasutomo Ota, Satoshi Iwamoto, and Yasuhiko Arakawa

Tuning growth of nanostructures can provide additional routes to engineer their characteristics. In this work, the authors report on a combined growth of GaSb/GaAs quantum dots (QDs) and growth of GaAs on (001) Ge substrate. Surface decorated with GaAs anti-phase domain is the initial template to investigate the growth-rate effects on the growth of self-assembled GaSb QDs. By varying the GaSb growth rates, QD ensembles with different morphologies are formed. Perpendicular alignment of elongated GaSb QDs is observed. Cross-sectional transmission electron microscopic images show a substantial reduction of lateral QD size when it is buried in GaAs matrix. Raman scattering as well as power-dependent photoluminescence spectroscopies are performed to reveal the optical properties of the nanostructures. Type-II band alignment characteristic is confirmed.

1. Introduction

Semiconductor nanostructures have gained significant attention as they are promising systems for realizing novel nanoelectronic and nanophotonic devices.^[1–3] Among nanostructures, quantum dot (QD) is highly interesting since it can confine carriers in three dimensions. The structural realization can simply be done via self-assembly. Intrinsic mismatch strain in heteroepitaxy acts as the driving force for QD formation process. Tuning the growth of self-assembled QDs can provide a simple route to fabricate QDs with desired characteristics for many device applications. Concerning photonic devices such as photodetectors and photovoltaic cells, wide and/or specific absorption band are the desired properties.^[4–7] In the past,

Zon, P. Phienlumert, S. Thainoi, Prof. S. Kanjanachuchai,
Prof. S. Ratanathamphan, Prof. S. Panyakeow
Semiconductor Device Research Laboratory (SDRL)
Department of Electrical Engineering
Faculty of Engineering
Chulalongkorn University
Bangkok 10330, Thailand
E-mail: s_panyakeow@yahoo.com

Prof. S. Kiravittaya
Advanced Optical Technology Laboratory (AOT Lab)
Department of Electrical and Computer Engineering
Faculty of Engineering
Naresuan University
Phitsanulok 65000, Thailand
E-mail: suwitki@nu.ac.th; suwitki@gmail.com


Dr. A. Tandaechanurat
International School of Engineering (ISE)
Faculty of Engineering
Chulalongkorn University
Bangkok 10330, Thailand

Dr. N. Nuntawong
National Electronics and Computer Technology Center (NECTEC)
National Science and Technology Development Agency (NSTDA)
Pathumthani 12120, Thailand

Dr. S. Sopitpan
Thai Microelectronics Center (TMEC)
National Science and Technology Development Agency (NSTDA)
Chachoengsao 24000, Thailand

V. Yordsri, Dr. C. Thanachayanont
National Metal and Materials Technology Center (MTEC)
National Science and Technology Development Agency (NSTDA)
Pathumthani 12120, Thailand

Prof. Y. Ota, Prof. S. Iwamoto, Prof. Y. Arakawa
Institute for Nano Quantum Information Electronics and Institute of
Industrial Science
The University of Tokyo
Tokyo 153-8505, Japan

 The ORCID identification number(s) for the author(s) of this article can be found under <https://doi.org/10.1002/pssa.201800499>.

DOI: 10.1002/pssa.201800499

we have made an attempt to integrate different nanostructures onto group-IV substrate aiming to realize novel combination of semiconductor heterostructures.^[8–11] Germanium is chosen in our study because it has a negligible lattice mismatch (<0.1%) to GaAs. Concerning the QD material, we are interested in type-II GaSb/GaAs QD since it has deep hole confinement potential and no electron confinement.^[5,6] Long carrier lifetime, which is a characteristic of type-II QD, has been proposed to be utilized in memory applications.^[12] GaSb/GaAs QD might also act as a model system to compare with widely studied type-I InAs/GaAs QD.^[1,2,12–14]

In this work, the growth-rate-dependent properties of GaSb/GaAs QDs grown on (001) Ge substrate are reported. The samples are grown by molecular beam epitaxy (MBE). The self-assembled GaSb/GaAs QDs are formed in Stranski–Krastanov mode. By varying the GaSb growth rate, circular and rectangular-based GaSb QDs are obtained. Cross-sectional transmission electron microscopy (TEM) shows the structure of buried GaSb QDs. Raman scattering and photoluminescence (PL) spectroscopies are carried out to reveal the optical properties. The characteristic of type-II band alignment is confirmed by analyzing the power-dependent PL properties.

2. Experimental Section

The samples are grown using a III–V MBE (RIBER, Compact 21TM) equipped with Sb valved cracker cell. Details of the sample preparation have been reported elsewhere.^[9–11] In brief, the growth is started with 500-nm GaAs buffer layer. Anti-phase domains (APDs) are typically formed due to the growth of polar GaAs on non-polar Ge substrate.^[15] After the buffer layer is grown, 3-monolayer (3-ML) GaSb is grown at 450 °C with a constant Sb flux of $\approx 5 \times 10^{-7}$ torr and with growth rates of 0.18, 0.14, 0.11, and 0.09 MLs⁻¹. The GaSb QDs is then capped with 20-nm GaAs at 350 °C and another 130 nm during the temperature ramp to 550 °C. The GaSb QD layer is grown again with the same growth conditions without capping for a surface morphology investigation by atomic force microscopy (AFM). The schematic diagram of the sample structure is shown in **Figure 1**.

The samples are characterized by AFM, TEM, Raman scattering, and PL. The AFM is done with Seiko SPA-400 in dynamic force mode in air. One low-growth-rate (0.11 MLs⁻¹) GaSb QD sample is selected for TEM investigation. The sample is prepared using Ar⁺ slicer and the sample is cut along the [110] direction. The cross-sectional structural investigation is

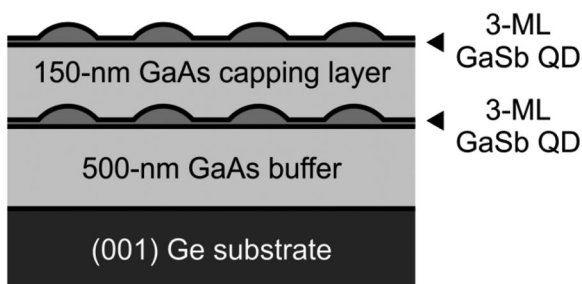


Figure 1. Schematic of the sample structure grown for this investigation. The GaSb growth rate is varied between 0.09 and 0.18 MLs⁻¹.

done by a 200-kV TEM machine (JEOL JEM-2010). The Raman scattering spectroscopy is performed at room temperature (RT) with a Raman spectrometer (Renishaw) equipped with 532-nm laser. PL spectroscopy is carried out with an in-house setup at a low temperature (20 K) using a He-cooled cryostat. The sample is excited by a 532-nm laser and the PL signal is collected by an InGaAs photodetector.

3. Results and Discussion

Figure 2 shows the surface morphologies of GaSb QDs on GaAs surface and their corresponding height histograms. After QD

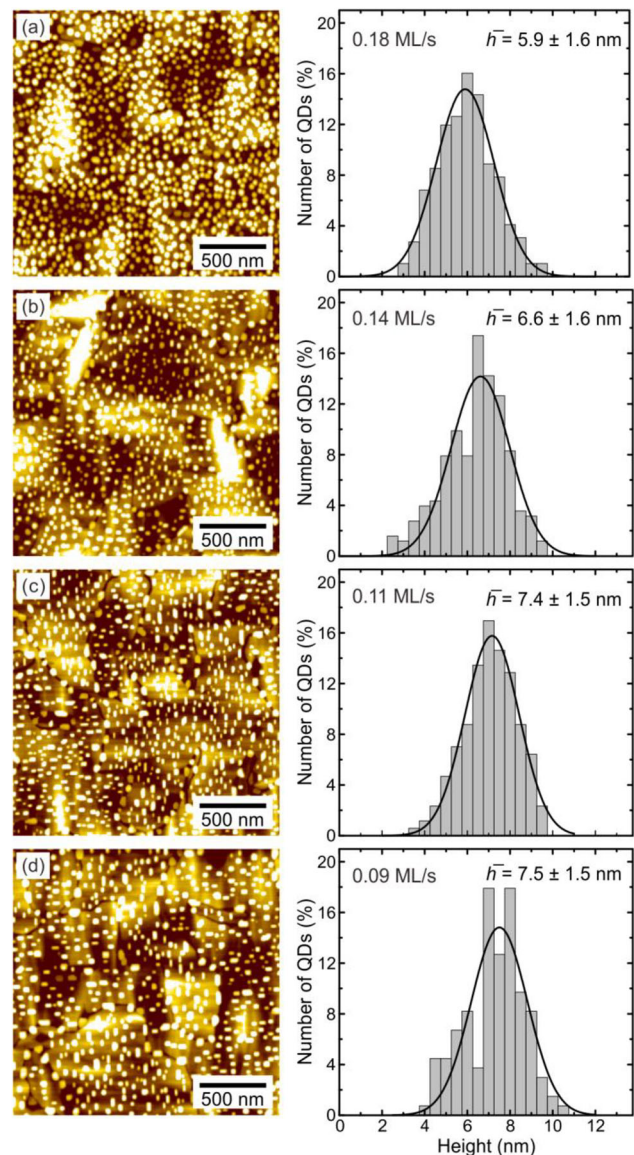


Figure 2. $2 \times 2 \mu\text{m}^2$ AFM images and the corresponding height histogram of GaSb/GaAs QDs grown on (001) Ge substrates by various GaSb growth rates of (a) 0.18, (b) 0.14, (c) 0.11, and (d) 0.09 MLs⁻¹. Height histograms are fitted Gaussian functions and the average and deviation values of the QD height are extracted and shown.

growth, we hardly observe the flat initial GaAs surface, which is decorated with APDs (see Figure S1, Supporting Information). The GaSb QD ensemble has a rather high areal coverage and the QD density is in the range of a few hundred QDs per μm^2 . The APD underneath is typically bounded with the nearby domains and anti-phase boundaries (APBs) are formed (see Figure S1, Supporting Information). The APB acts as preferential nucleation positions for InSb QD with some specific growth conditions.^[11] For GaSb/GaAs QDs grown under the conditions described above, the APBs seem to have no effect on GaSb QD nucleation position as observed in the AFM images in Figure 2. When the growth rate decreases, the QD density gradually decreases and the QDs become larger (both height and lateral size). Average QD height increases from 5.9 to 7.5 nm when the growth rate decreases from 0.18 to 0.09 MLs^{-1} . This trend is general for many QD systems, for example, InAs/GaAs QDs.^[16,17] However, if one looks closer at the shape of GaSb QDs, one can observe an elongation of the QDs which becomes more pronounced as growth rate decreases. **Figure 3(a,b)** are the magnified 3D AFM images of a typical GaSb QD grown at a high (0.18 MLs^{-1}) and a low (0.09 MLs^{-1}) growth rates. Generally, the QDs grown at high growth rates show a circular based shape while those grown at low growth rates show an elongated, rectangular based shape. This anisotropic QD shape may originate from surface reconstruction which depends on growth

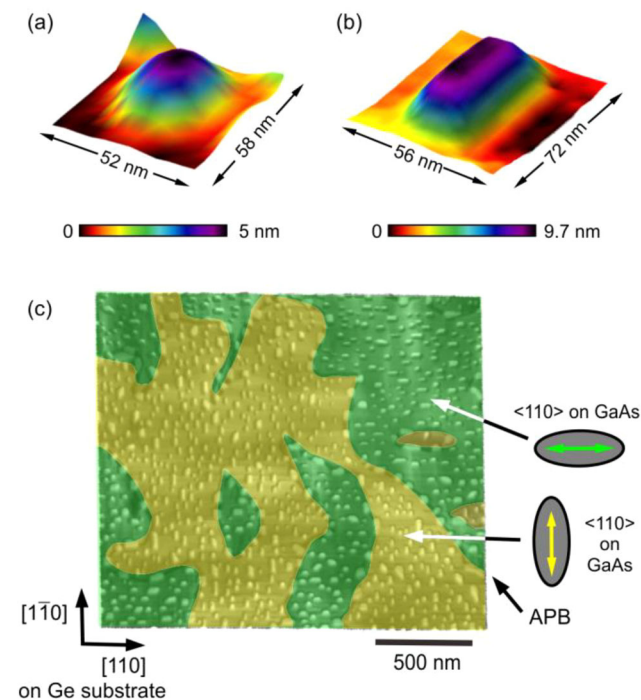


Figure 3. Magnified 3D perspective AFM images of GaSb/GaAs QDs grown (a) high growth rate (0.18 MLs^{-1}) and (b) low growth rate (0.09 MLs^{-1}). c) 3D AFM image of GaSb/GaAs QDs grown at the growth rate of 0.11 MLs^{-1} . Different perpendicular GaAs APDs are highlighted with yellow and green shading. Obviously perpendicular QD elongation directions are observed and attributed to the locally $\langle 110 \rangle$ oriented GaAs surface.

rates and the V/III flux ratio. Since atomic surface structure has a lower symmetry than the crystal structure, the elongated QD structure is expected. With an additional growth of GaSb on GaAs substrate (see Figure S2, Supporting Information) and previous reports,^[14,18] we can confidentially identify the GaSb QD elongation direction as the $[110]$ direction. Since the GaAs APDs on (001) Ge substrate are orthogonal, the observed elongation of GaSb QDs can act as a local probe for GaAs crystalline direction. To illustrate this fact, an APD-highlighted AFM image of the surface covered with low-growth-rate (0.11 MLs^{-1}) elongated GaSb QDs is shown in Figure 3(c). An array of elongated QDs along two perpendicular directions ($[110]$ and $[\bar{1}\bar{1}0]$) might have unique optical characteristics, which is a subject of our future investigations.

Capping process does also affect the QD structures.^[18,19] We therefore investigate our buried GaSb QDs by cross-sectional TEM. **Figure 4** shows cross-sectional TEM images of the selected sample, which contains low-growth-rate GaSb QDs. Figure 4(a) shows the overview of the sample cross-section. One can clearly

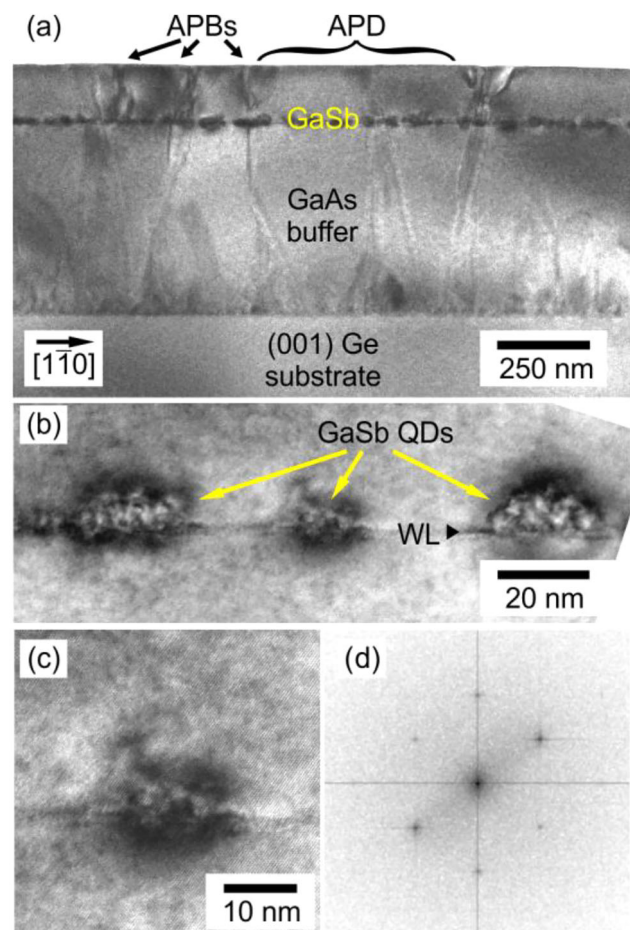


Figure 4. a) Overview cross-sectional TEM image observed in $[110]$ direction. b) The high magnification TEM image showing three nearby GaSb QDs on WL. c) The high-resolution TEM image of single GaSb QD. d) The Fourier transform image of (c) showing zinc-blende atomic arrangement in spatial frequency domain.

observe threading dislocation in the GaAs buffer and capping layers. Typically, the dislocation density decreases and the surface becomes more flat when thick GaAs buffer is grown. The buried GaSb QD layer is clearly observed as it has very high contrast (due to high strain and large atomic size). In the cross-sectional TEM image, APD is a flat area between dislocation lines and the APBs are the end of dislocation lines terminating at the surface. Since most of GaSb QDs are on the APDs, we concentrate our investigation on them. Figure 4(b) shows three nearby GaSb QDs. Each QD is dome-shaped and looks rather different from the cross-sections of QDs on GaAs surface. The high strain contrast areas indicate the GaSb QD regions. They lie on a flat GaSb wetting layer (WL). The observed QDs have the height of $\approx 5\text{--}10\text{ nm}$ and lateral size of $\approx 15\text{--}30\text{ nm}$. The former is consistent with the AFM result whereas the latter is much smaller. The discrepancies are due in parts to AFM tip convolution and the Sb-As intermixing during capping which may shrink buried QDs.^[18–20] Closer looks into the TEM images of large GaSb QDs, we observe a few misfit dislocations. Therefore, the strain of the large GaSb QD is relaxed. Such defect is formed due to the second strain relaxation after QD formation. However, we observed no misfit defect for small GaSb QDs. One example is shown in Figure 4(c). In Figure 4(d), Fourier transform image of the TEM image is presented in order to confirm the coherency of buried GaSb atoms in GaAs matrix. This result indicates that the buried QD array comprises both defective and defect-free GaSb QDs. Unfortunately, the statistical ratio can not be drawn due to the small number of QDs in the high-resolution TEM images.

In order to evaluate the trend of residual strain in GaSb/GaAs QDs, Raman scattering analysis is performed. Figure 5(a) shows the Raman scattering spectra obtained from samples with GaSb QDs grown at different growth rates. Typical transverse-optical (TO) and longitudinal-optical (LO) phonon peaks of GaAs are observed at ≈ 268 and $\approx 291\text{ cm}^{-1}$, respectively.^[10] The GaSb-related peaks are observed in the range between 220 and 240 cm^{-1} . After background subtraction, the GaSb-related peaks are well fitted with two Gaussian functions as shown in Figure 5(b). We attribute the peaks at $234\text{--}236\text{ cm}^{-1}$ to GaSb LO phonons and the peaks at $226\text{--}228\text{ cm}^{-1}$ to GaSb TO phonons. The gradual redshift of TO GaSb peak is observed when the growth rate is reduced. It corresponds to slightly higher average tensile strain in low-growth rate QDs. This observation might be due to the contribution of large relaxed GaSb QDs which contain misfit dislocations. Since the low-growth-rate QD array has higher density of large relaxed QD (see Figure 2), the ratio of relaxed QDs to the coherent ones is expected to be higher in the array. The dislocation formed by the strain relaxation in the QD does generally create highly tensile strain area.^[21] It therefore results in the redshift of TO GaSb peak.

Optical properties of buried GaSb/GaAs QDs grown at different growth rates are probed by PL spectroscopy. Figure 6 shows the PL spectra of GaSb QDs at 20 K. The PL emission from all samples are in the near IR range ($1000\text{--}1200\text{ nm}$). For small QDs grown at high growth rate (e.g., 0.18 ML s^{-1}), the emission shows a slight blueshift as compared with low-growth-rate QDs (e.g., 0.09 ML s^{-1}). The PL linewidths or full-width-at-half-maxima are rather broad ($58\text{--}113\text{ meV}$). We attribute them

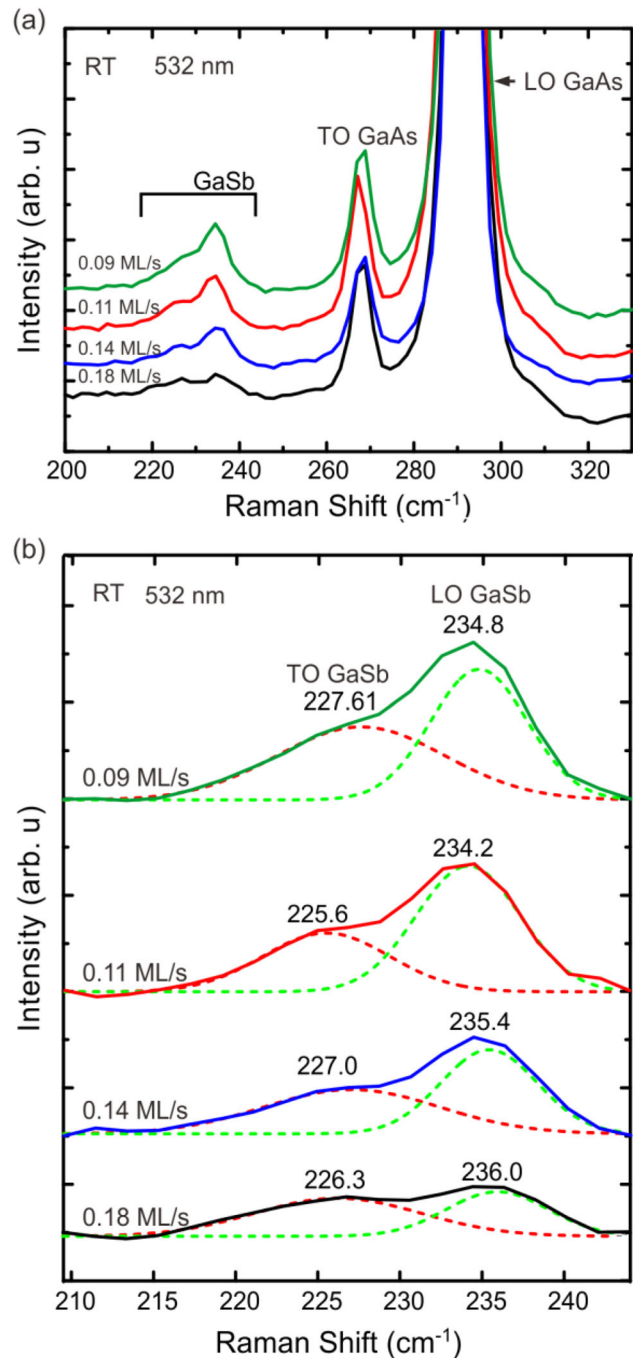


Figure 5. a) RT Raman scattering spectra of samples containing buried GaSb and uncapped GaSb QDs grown at different growth rates. The spectra show both GaAs and GaSb-related peaks. b) The Raman scattering spectra described the LO and TO GaSb-related peaks. The dash lines are from Gaussian fits. Labels are the peak positions as extracted from the fits.

to the inhomogeneous broadening due to the large size fluctuation as well as substantial Sb-As intermixing during the growth and capping of these QDs. This large inhomogeneous broadening might be a desired characteristic for QD devices operating in broad IR wavelength range. However, due to

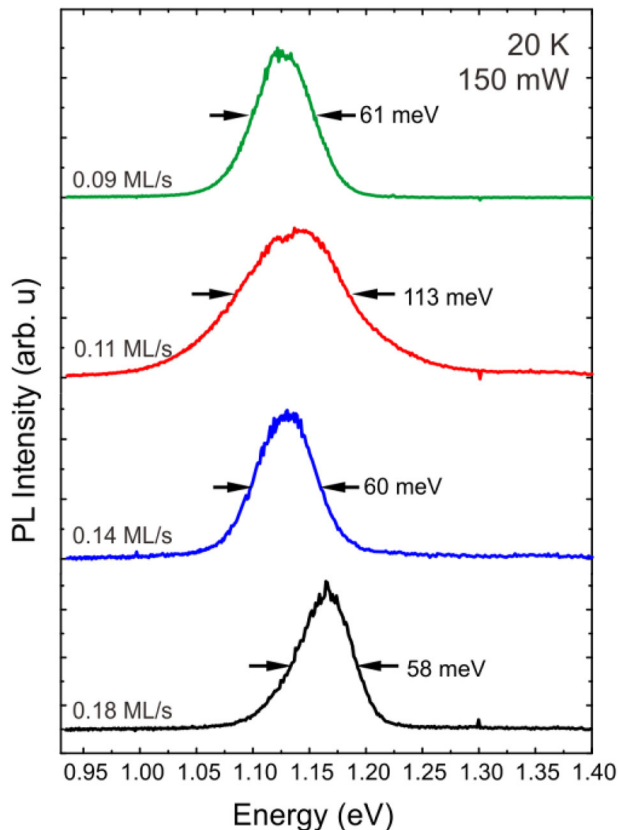


Figure 6. Low-temperature (20 K) PL spectra showing PL emission from GaSb QD ensembles grown at different growth rates. The PL linewidths are indicated.

this fact, the expected small differences on the optical properties of the isotropic and anisotropic (circular vs. rectangular based) QD shapes cannot be resolved. Polarization dependent PL is needed for deeper understanding the properties of these QDs.^[22,23]

In order to confirm the type-II band alignment in GaSb/GaAs QDs, the low-temperature power-dependent PL spectroscopies are performed for all samples. As an example, the spectra from GaSb/GaAs QDs grown at a low growth rate of 0.09 ML s^{-1} is shown in **Figure 7(a)**. The spectra show a clear blueshift with increasing PL intensity when the excitation power is increased. This blueshift qualitatively agrees with the bending of the band diagram shown as the inset of **Figure 7(a)**. When the carrier density is increased, the Coulomb attractive force between electrons and confined holes becomes stronger and it induces a triangular potential around the QD.^[24] This produces weakly confined electronic states around the QD and the quantized energy levels for electrons. It results in a blueshift of PL emission when the excitation power increases. **Figure 7(b)** shows the summarized peak shifts of all investigated samples as a function of cubic root of excitation laser power P (i.e., $P^{1/3}$). According to the theoretical analysis,^[24] the linear relation is expected and it is confirmed in this plot. We therefore conclude that our GaSb/GaAs QDs grown on (001) Ge substrate have type-II band alignment.

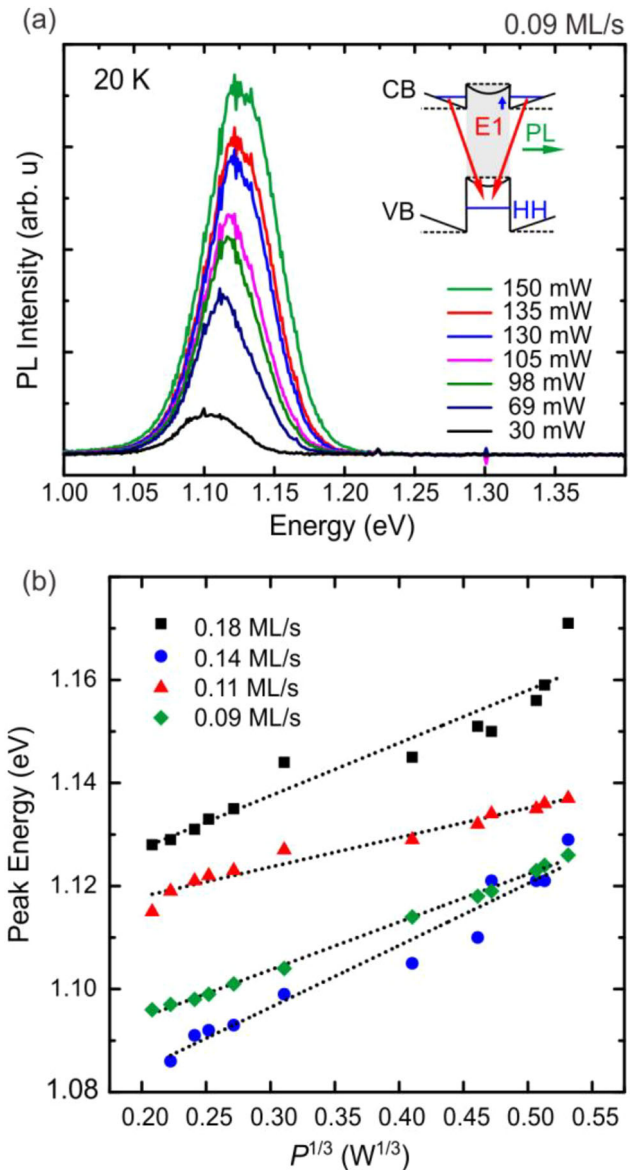


Figure 7. a) The power-dependent PL spectra showing the blueshift of PL emission from GaSb QD ensembles. Inset of (a) shows schematic band diagrams of GaSb/GaAs QD at low and high excitation as dashed and solid lines. b) The extracted peak energies of GaSb QD peaks as a function of cubic root of excitation power ($P^{1/3}$). Experimental data are well fitted with linear function (dotted lines) indicating the type-II band alignment of GaSb/GaAs QDs.

4. Conclusion

We present our investigation of GaSb/GaAs QDs grown at different growth rates on (001) Ge substrate. Morphological difference between the high-growth-rate and the low-growth-rate QDs are observed. The elongated GaSb QDs obtained by the growth at low growth rates can act as a local probe of the GaAs crystalline direction of each APD. Cross-sectional TEM is applied to investigate the buried QD structure. Analysis of Raman scattering spectra reveals a slightly different residual strain in the GaSb QDs. The PL emission from GaSb/GaAs QDs indicates a

single dominant peak with a large inhomogeneous broadening. The power-dependent PL confirms the type-II band alignment of our GaSb/GaAs QDs on Ge substrate. This results enhance the understanding on the relations between QD growth conditions and the obtained QD characteristics especially for the growth of III–V nanostructure on group-IV substrate.

Supporting Information

Supporting Information is available from the Wiley Online Library or from the author.

Acknowledgements

This study was supported by the Research Chair Grant, the National Science and Technology Development Agency (NSTDA), Thailand (Contract No. FDA-CO-2558-1407-TH), Asian Office of Aerospace Research and Development (AOARD) Grant, co-funded with Office of Naval Research Global (ONRG), under Grant No. FA 2386-16-1-4003, Thailand Research Fund (Contract No. DPG5380002), NANOTEC, NSTDA, Thailand (Contract No. RES_50_016_21_016), and Chulalongkorn University. Ms. Zon acknowledges the support from ASEAN University Network/Southeast Asia Engineering Education Development Network (AUN/SEED-Net) (Contract No. CU-58-051-EN). Mr. Visittapong Yordsri and Dr. Chanchana Thanachayanont thank JEOL Ltd. for the access of Ionlicer-JEOL machine in the course of TEM sample preparation.

Conflict of Interest

The authors declare no conflict of interest.

Keywords

GaSb/GaAs, Ge substrate, molecular beam epitaxy, quantum dots

Received: June 30, 2018

Revised: September 2, 2018

Published online: October 8, 2018

- [1] M. Henini, *Handbook of Self Assembled Semiconductor Nanostructures for Novel Devices in Photonics and Electronics*, Elsevier Science, Oxford **2008**.
 [2] D. Bimberg, *Semiconductor Nanostructures*, Springer, Berlin **2008**.
 [3] Y. Arakawa, H. Sakaki, *Appl. Phys. Lett.* **1982**, *40*, 939.
 [4] S. Sengupta, S. Chakrabarti, *Structural, Optical and Spectral Behaviour of InAs-Based Quantum Dot Heterostructures: Applications*

for High-Performance Infrared Photodetectors, Springer, Singapore **2018**.

- [5] W.-H. Lin, C.-C. Tseng, K.-P. Chao, S.-C. Mai, S.-Y. Kung, S.-Y. Wu, S.-Y. Lin, M.-C. Wu, *IEEE Photon. Technol. Lett.* **2011**, *23*, 106.
 [6] A. Kechiantz, A. Afanasev, J.-L. Lazzari, *Prog. Photovoltaics Res. Appl.* **2015**, *23*, 1003.
 [7] R. B. Laghumavarapu, B. L. Liang, Z. S. Bittner, T. S. Navruz, S. M. Hubbard, A. Norman, D. L. Huffaker, *Solar Energy Mater. Solar Cell* **2013**, *114*, 165.
 [8] W. Tantiweerasophon, S. Thainoi, P. Changmuang, S. Kanjanachuchai, S. Rattanathammaphan, S. Panyakeow, *J. Cryst. Growth* **2011**, *323*, 254.
 [9] Zon, T. Poempool, S. Kiravittaya, S. Sopitpan, S. Thainoi, S. Kanjanachuchai, S. Ratanathammaphan, S. Panyakeow, *MRS Adv.* **2016**, *1*, 1729.
 [10] Zon, T. Poempool, S. Kiravittaya, N. Nuntawong, S. Sopitpan, S. Thainoi, S. Kanjanachuchai, S. Ratanathammaphan, S. Panyakeow, *Electron. Mater. Lett.* **2016**, *12*, 517.
 [11] Zon, T. Poempool, S. Kiravittaya, S. Sopitpan, S. Thainoi, S. Kanjanachuchai, S. Ratanathammaphan, S. Panyakeow, *J. Cryst. Growth* **2017**, *468*, 541.
 [12] M. Geller, C. Kapteyn, L. Müller-Kirsch, R. Heitz, D. Bimberg, *Phys. Stat. Sol. (b)* **2003**, *238*, 258.
 [13] B. R. Bennett, P. M. Thibado, M. E. Twigg, E. R. Glaser, R. Magno, B. V. Shanabrook, L. J. Whitman, *J. Vac. Sci. Technol.* **1996**, *14*, 2195.
 [14] G. Balakrishnan, J. Tatebayashi, A. Khoshakhlagh, S. H. Huang, A. Jallipalli, L. R. Dawson, D. L. Huffaker, *Appl. Phys. Lett.* **2006**, *89*, 161104.
 [15] Y. Li, G. Salviati, M. M. G. Bongers, L. Lazzarini, L. Nasi, L. J. Giling, *J. Cryst. Growth* **1996**, *163*, 195.
 [16] Y. Nakata, K. Mukai, M. Sugawara, K. Ohtsubo, H. Ishikawa, N. Yokoyama, *J. Cryst. Growth* **2000**, *208*, 93.
 [17] V. G. Dubrovskii, V. A. Egorov, G. E. Cirlin, N. K. Polyakov, Y. B. Samsonenko, N. V. Kryzhanovskaya, A. F. Tsatsul'nikov, V. M. Ustinov, *Semiconductor* **2003**, *37*, 883.
 [18] K. Yamaguchi, *Handbook of Self Assembled Semiconductor Nanostructures for Novel Devices in Photonics and Electronics* (Ed: M. Henini), Elsevier Science, Oxford **2008**, Ch. 8.
 [19] A. J. Martin, J. Hwang, E. A. Marquis, E. Smakman, T. W. Saucer, G. V. Rodriguez, A. H. Hunter, V. Sih, P. M. Koenraad, J. D. Phillips, J. Millunchick, *Appl. Phys. Lett.* **2013**, *102*, 113103.
 [20] R. Songmuang, S. Kiravittaya, O. G. Schmidt, *J. Cryst. Growth* **2003**, *249*, 416.
 [21] J. P. Hirth, J. Lothe, *Theory of Dislocations*, 2nd ed., Wiley, New York **1982**.
 [22] T. Kawazu, T. Noda, T. Mano, Y. Sakuma, H. Sakaki, *Jpn. J. Appl. Phys.* **2012**, *51*, 115201.
 [23] T. Chokamnuai, P. Rattanadon, S. Thainoi, S. Panyakeow, S. Kanjanachuchai, *J. Cryst. Growth* **2013**, *378*, 524.
 [24] N. N. Ledentsov, J. Böhrer, M. Beer, F. Heinrichsdorff, M. Grundmann, D. Bimberg, *Phys. Rev. B* **1995**, *52*, 14058.